



Immunometabolic Network Interactions of the Kynurenine Pathway in Cutaneous Malignant Melanoma

Soudabeh Rad Pour^{1*}, Hiromasa Morikawa², Narsis A. Kiani^{1,3}, David Gomez-Cabrero^{1,4}, Alistair Hayes⁵, Xiaozhong Zheng⁵, Maria Pernemalm⁶, Janne Lehtiö⁶, Damian J. Mole⁵, Johan Hansson^{6,7}, Hanna Eriksson^{6,7} and Jesper Tegnér^{1,2,3}

¹ Unit of Computational Medicine, Department of Medicine, Centre for Molecular Medicine, Karolinska Institute, Stockholm, Sweden, ² Biological and Environmental Sciences and Engineering Division (BESE), Computer, Electrical, and Mathematical Sciences and Engineering Division (CEMSE), King Abdullah University of Science and Technology (KAUST), Thuwal, Saudi Arabia, ³ Unit of Computational Medicine, Algorithmic Dynamics Lab, Department of Medicine Solna, Centre for Molecular Medicine, Karolinska Institute and SciLifeLab, Stockholm, Sweden, ⁴ Navarrabiomed, Complejo Hospitalario de Navarra (CHN), Universidad Pública de Navarra (UPNA), IdiSNA, Pamplona, Spain, ⁵ MRC Centre for Inflammation Research, Queen's Medical Research Institute, University of Edinburgh, Edinburgh, United Kingdom, ⁶ Department of Oncology-Pathology, Karolinska Institute, Stockholm, Sweden, ⁷ Department of Oncology/Skin Cancer Center, Theme Cancer, Karolinska University Hospital, Stockholm, Sweden

OPEN ACCESS

Edited by:

Peter Jon Nelson,
Ludwig Maximilian University of
Munich, Germany

Reviewed by:

Jian Jian Li,
University of California, Davis,
United States
Liwei Lang,
Augusta University, United States

*Correspondence:

Soudabeh Rad Pour
soudabeh.rad-pour@ki.se

Specialty section:

This article was submitted to
Cancer Metabolism,
a section of the journal
Frontiers in Oncology

Received: 06 September 2019

Accepted: 13 January 2020

Published: 03 February 2020

Citation:

Rad Pour S, Morikawa H, Kiani NA, Gomez-Cabrero D, Hayes A, Zheng X, Pernemalm M, Lehtiö J, Mole DJ, Hansson J, Eriksson H and Tegnér J (2020) Immunometabolic Network Interactions of the Kynurenine Pathway in Cutaneous Malignant Melanoma. *Front. Oncol.* 10:51. doi: 10.3389/fonc.2020.00051

Dysregulation of the kynurenine pathway has been regarded as a mechanism of tumor immune escape by the enzymatic activity of indoleamine 2, 3 dioxygenase and kynurenine production. However, the immune-modulatory properties of other kynurenine metabolites such as kynurenic acid, 3-hydroxykynurenine, and anthranilic acid are poorly understood. In this study, plasma from patients diagnosed with metastatic cutaneous malignant melanoma (CMM) was obtained before (PRE) and during treatment (TRM) with inhibitors of mitogen-activated protein kinase pathway (MAPKs). Immuno-oncology related protein profile and kynurenine metabolites were analyzed by proximity extension assay (PEA) and LC/MS-MS, respectively. Correlation network analyses of the data derived from PEA and LC/MS-MS identified a set of proteins that modulate the differentiation of Th1 cells, which is linked to 3-hydroxykynurenine levels. Moreover, MAPKs treatments are associated with alteration of 3-hydroxykynurenine and 3hydroxyanthranilic acid (3HAA) concentrations and led to higher “CXCL11,” and “KLRD1” expression that are involved in T and NK cells activation. These findings imply that the kynurenine pathway is pathologically relevant in patients with CMM.

Keywords: kynurenine pathway, cutaneous malignant melanoma, immune metabolic network interactions, 3-hydroxykynurenine, CD4+ T helper (Th) cells

INTRODUCTION

Cutaneous malignant melanoma (CMM) is the most common form of melanomas and arises from a malignant transformation of melanocytes (1). The 5-year relative survival rate for patients with stage I CMM is more than 95%, while until recently, median survival was only 6–9 months in stage IV disease (1). Targeting the oncogenic mitogen-activated protein kinase (MAPK) pathway with small molecule inhibitors, i.e., BRAF and/or MEK inhibitors (MAPK-inhibitors; MAPKIs),

has led to improved overall survival (OS) and progression-free survival (PFS) in patients with BRAF-mutant CMM (2).

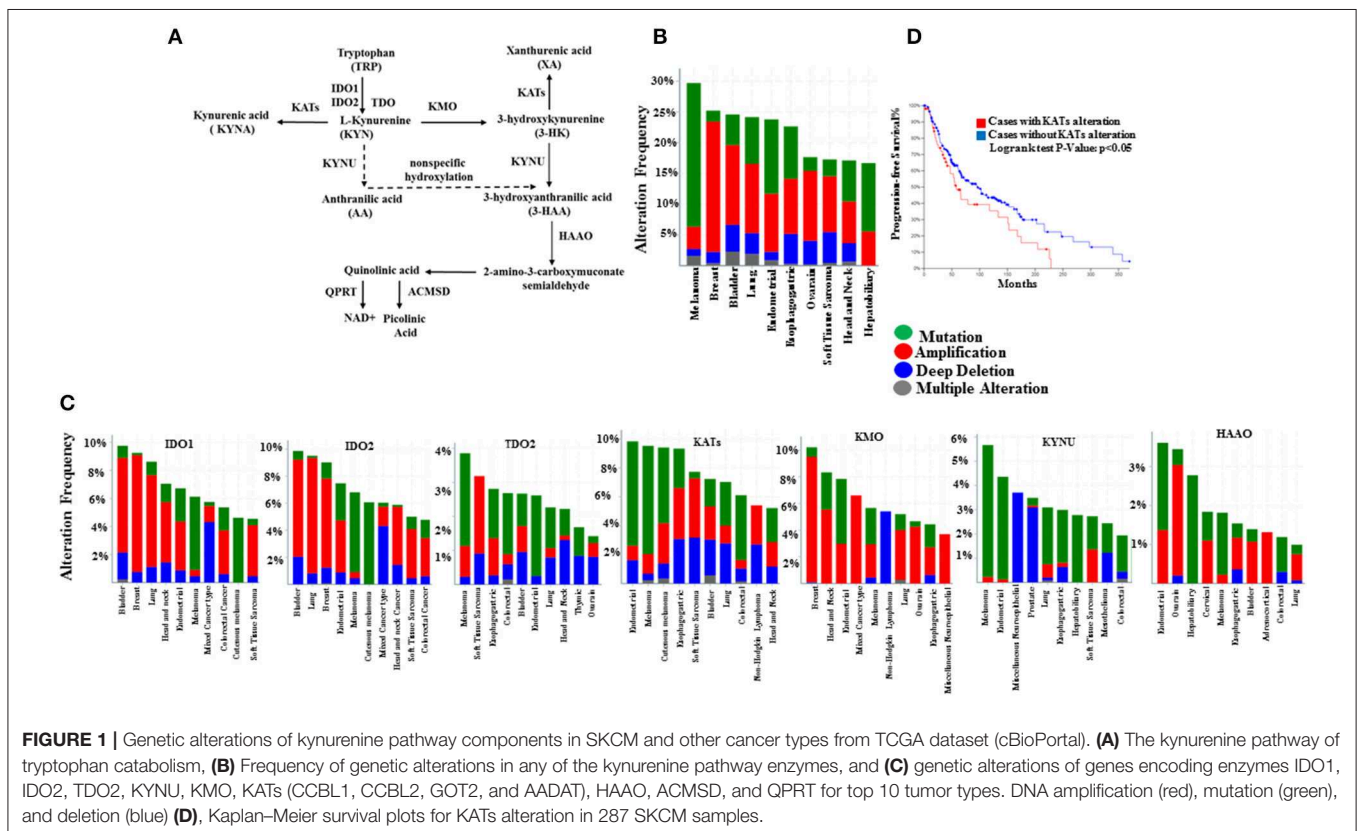
It has been shown that patients with advanced CMM receiving immune checkpoint inhibitors (ICPIs), targeting the immunosuppressive programmed cell death 1 receptor (PD-1) have favorable response rate (33–44%). However, approximately two-thirds of patients do not have a satisfactory response to ICPIs (3–6). More recently, preliminary results in patients with metastatic melanoma indicate that combining indolamine 2, 3-dioxygenase 1 inhibitors (IDO1i) with either CTLA-4 inhibitor or PD-1 inhibitor (PD-1i) increases the effectiveness of these immunotherapies in CMM patients (7–9). Though, in (ECHO-301/Keynote-252), randomized controlled trial in patients with metastatic melanoma, combination treatment with an IDO1 inhibitor, epacadostat, and the PD-1i, pembrolizumab, did not show any improvement of survival compared to single therapy with PD-1i (10).

MAPK dysregulation led to differential antitumor immune response, which involves in Th1 signaling and cytotoxic effect (11, 12). The beneficial immunologic effects of MAPKs have previously demonstrated. For instance, MAPKs induces immunologic changes in tumor cells such as higher MHCs expression, and tumor-associated antigens (13, 14). MAPKs also lowers the induction of immunosuppressive cytokines such as IL-10, VEGF, or IL-6 (15, 16). Interestingly, immunomodulatory effects of MAPKs, in combination with immune checkpoint inhibitors, emerge as a promising strategy in cancer therapy (17).

On the other hand, targeting some metabolic substances synergizes with MAPK inhibition and delays the onset of drug resistance in melanoma (18). Therefore, targeting metabolic pathway might enhance the impact of MAPK inhibitors. Combining IDO1i, which is an effector of the Kynurenine pathway (KP), with immune checkpoint blockaders has been used in order to improve the effectiveness of these immunotherapies.

KP activation leads to tryptophan (TRP) metabolism and therefore generation of multiple immunomodulatory metabolites, known as Kynurenine pathway metabolites (KPM) including kynurenine (KYN), anthranilic acid (AA), kynurenic acid (KYNA), 3-hydroxykynurenine (3-HK), 3hydroxyanthranilic acid (3HAA), xanthurenic acid (XA) and culminates in the biosynthesis of nicotinamide adenine dinucleotide (NAD+) (Figure 1A) (19). The activity of the KP associated enzymes defined by the concentrations of direct derivatives of the metabolites, for instance the KYN: TRP ratio is used as an index of IDO activity (20–23).

KPMs have been measured using sensitive methods such as liquid chromatography-tandem mass spectrometry (LC-MS/MS). Except 3HAA, other KPMs are stable. 3HAA is known to be particularly unstable over time and sensitive to light (20, 24). It has been reported that accumulation of KYN induces T- B- and natural killer (NK)- cells apoptosis (25). The concentration of different metabolites in the KP is controlled by groups of enzymes such as IDO1, IDO2, and tryptophan 2, 3-dioxygenase (TDO2),



three rate-limiting enzymes that catalyze the cleavage of TRP into KYN (26–28).

KYN itself is a substrate for different enzymes with immunomodulatory properties along KP. Enzymes such as kynurenine 3-monooxygenase (KMO) and kynurenine aminotransferases (CCBL1, AADAT, CCBL2, and GOT2; collectively called KATs) that convert KYN to 3-HK and KYNA, respectively (Figure 1A) (29–31).

It has been shown that KP activity is elevated in patients in numerous types of cancer (32–39). Moreover, the expression of IDO1 by tumor cells has been regarded as an essential immune escape mechanism that suppresses T cell activity (40, 41) through mTORC1 triggering autophagy (42, 43). Likewise, induction of IDO1 by inflammatory cytokines, including IFN γ and tumor necrosis factor α (TNF- α), has been linked to poor prognosis in CMM as well as various different cancer types (44, 45). It is also reported that plasma levels of KYN, 3-HK, and KYNA are associated with more aggressive forms of breast cancer and glioblastoma (38, 46). However, this has not been conclusively shown in CMM patients. Furthermore, whether KP metabolic dysregulation occurs in patients treated with MAPKIs was not known yet. Therefore, we undertook this study to evaluate immune-metabolic network interactions of the KP in CMM to explore the link between KPMs and regulation of the antitumor immune response. We measured the plasma levels of KPMs and immune-related proteins, using LC-MS/MS and proximity extension assay (PEA), respectively, in healthy individuals and, CMM patients before and during treatment with MAPKIs.

MATERIALS AND METHODS

Cell Culture

Parental A375 BRAF V600E-mutated human melanoma cell line and daughter cell line with induced BRAFi resistance [vemurafenibR4 resistant subline (A375R)] were obtained from Professor Johan Hansson's research group.

Cell lines were cultured for 48 h for KPMs measurement at a density of 1.0×10^4 cells/ml in RPMI 1640 medium (Gibco) supplemented with 10% heat-inactivated fetal bovine serum (Gibco) in the presence of IFN γ (50 ng/mL) and TNF α (10 ng/mL).

Reagents

Recombinant IFN γ (cat. 285-IF-100) and TNF- α (cat. 210-TA7CF) were purchased from R&D system (McKinley Place NE).

Cell Lines Authentication

We received early passages of parental A375 cells and the daughter BRAFi resistant subline and no changes in phenotype or morphology was observed. Furthermore, mycoplasma testing was routinely performed (LookOut Mycoplasma PCR Detection kit, Sigma Aldrich, MP0035), verifying that the cells were mycoplasma free (Supplementary Figure 10).

Plasma Sampling and Sample Collection

Plasma samples were collected before (PRE) and during treatment between day 21–28 (TRM) from melanoma patients

with disseminated (M1c and M1b) disease, undergoing first-line therapy with MAPKIs (Table 1, Supplementary Tables 1A, 3). Blood was obtained from five patients, collected in EDTA tubes and centrifuged at $1,500 \times g$ for 10 min within 1 h after collection. Separated plasma was centrifuged at $2,400 \times g$ for 15 min and was frozen at -70°C within 1 h of processing. Samples were then shipped overnight on dry ice for analysis. All samples were stored at -70°C until they were assayed. The sample collection was conducted by Good Clinical Practice/the Declaration of Helsinki with informed consent from all patients and was approved by the Stockholm Regional Ethics Committee, Karolinska Institute, Sweden.

Healthy Volunteers

Plasma was collected from five healthy volunteers at the Karolinska University Hospital to be used as healthy controls, and all donors gave their informed consent before participating. Only volunteers over the age of 18 years were included in the control set (Supplementary Table 1B). Those with the presence of any of the following conditions were excluded: renal dysfunction, hepatic dysfunction (Child-Pugh score B or C), pregnancy or breastfeeding, immune-mediated inflammatory disease or medications, blood dyscrasia or anemia.

Liquid Chromatography-Tandem Mass Spectrometry (LC-MS/MS) for Analysis of Tryptophan Metabolites

Plasma samples were diluted at a 1:1 ratio with 4% phosphoric acid (in HPLC grade H₂O), and internal standard(s) was added as appropriate (e.g., 50 ng deuterated tryptophan; d5-TRP). To allow quantification, a calibration curve was made using an array of aqueous standards prepared by serial dilution (100, 50, 20, 10, 5, 2, 1, 0.5, 0.2, and 0.1 ng) of the following compounds: tryptophan, kynurenine, kynurenic acid, 3-hydroxykynurenine, anthranilic acid, 3hydroxyanthranilic acid, quinolinic acid and xanthurenic acid. These standards were suspended in 1% bovine serum albumin as a surrogate plasma matrix, and the internal standard(s) (e.g., 50 ng d5-TRP or d5-KA) were added before a 1:1 dilution in 4% phosphoric acid (in HPLC grade H₂O). Each sample and the aqueous standard was transferred to a well in a 96-well analyte extraction plate (H₂O Oasis HLB, 10 mg sorbent, 30 μm particle size) and vacuumed to dryness, washed and dried. Extracts were washed with H₂O and eluted with 80% methanol (in HPLC grade H₂O.) The elute dried by nitrogen gas flow at 60°C and 30 L/min. Dried extracts were re-suspended in 100 μl 30% methanol in HPLC grade H₂O. Ten microliter volumes of each suspended extract were injected onto a column (Ace C18-PFP column; 100×2.1 mm internal diameter, 1.7 μm) using a Shimadzu Nexera MP UHPLC liquid chromatography system linked to a QTRAP 6500 mass spectrometer (Sciex). The flow rate was set at 0.4 ml/min at 40°C . The separation was carried out using mobile phase A—0.1% formic acid (in HPLC grade H₂O) and mobile phase B—0.1% formic acid (in methanol). Data were acquired and processed using Analyst 3.0 software ABI (Sciex).

TABLE 1 | Clinical characterization of melanoma patients.

	Age	Gender	Primary	BRAF status	PFS ^a (days)	OS ^b (days)	Disease stage	Treatment response	Type of treatment
1	60	Male	CMM ^c	V600E	186	696	M1c ^d	PR ^e	BRAF ^f
2	50	Female	CMM	V600E	170	637	M1c	PR	BRAF ⁱ
3	32	Male	UK ^g	V600E	148	248	M1c	PR	BRAF ⁱ
4	40	Male	CMM	V600E	101	203	M1c	PR	BRAF ⁱ ,
5	43	Female	CMM	V600E	562	Alive	M1c	PD ^h	BRAF ⁱ and MEK ⁱ

^aProgression-free survival (PFS).

^bOverall survival (OS).

^cCutaneous malignant melanoma (CMM).

^dCutaneous or, subcutaneous metastases (M1c).

^ePartial response (PR).

^fBRAF inhibitor (BRAFi; Dabrafenib/Vemurafenib).

^gUnknown (UK).

^hProgressive disease (PD).

ⁱMEK inhibitor (MEKi; Binimetinib).

Mass Spectrometry Analysis of Parental A375 BRAF V600E-Mutated Human Melanoma Cell Line and of Daughter Cell Lines With Induced BRAFi Resistance

The detail was described previously (47).

Plasma Protein Detection

Plasma samples were analyzed using proximity extension assay (PEA) at the clinical biomarkers facility at SciLifeLab, Uppsala, Sweden. Ninety two human protein biomarkers were measured using Olink[®] ImmunoOnc I panel (Olink Proteomics, Uppsala, Sweden). Measurements were performed using 1 μ L of each sample. In PEAs, a pair of oligonucleotide-conjugated antibodies bind to their targeted protein in the samples. When the two probes are in close proximity, the oligonucleotides will hybridize in a pair-wise manner. The addition of a DNA polymerase leads to a proximity-dependent DNA polymerization event, generating a unique PCR target sequence. The target sequence is detected and quantified using a microfluidic real-time PCR instrument (Biomark HD, Fluidigm). The Olink protocol has been described in detail by Assarsson et al. (48). Data is then quality controlled and normalized using an internal extension control and an inter-plate control, to adjust for intro- and inter-run variation. The final assay readout is presented in Normalized Protein expression (NPX) values, which is an arbitrary unit on a log₂-scale where a high value corresponds to higher protein expression. More details on the assay detection limits, intra- and inter-assay precision data are available on the manufacturer's website (www.olink.com) (48).

TCGA Analyses

Mutations, copy-number alterations, and mRNA and protein expression profile of KP enzymes (IDO1/2, TDO2, KMO, KYNU, CCBL1/2, GOT2, AADAT, and ACMSD) in TCGA (provisional) cohort data accessed at cBioPortal for Cancer Genomics in January 2018, <http://www.cbioportal.org>.

cBioPortal delivers genomic datasets for 24 cancer diagnoses (<http://www.cbioportal.org/>). The following tumor types were selected: adrenocortical carcinoma ($n = 92$), cholangiocarcinoma ($n = 51$), bladder urothelial cancer ($n = 413$), colorectal adenocarcinoma ($n = 640$), breast cancer ($n = 1,105$), glioma ($n = 1,136$), cervical cancer ($n = 308$), stomach adenocarcinoma ($n = 664$), uveal melanoma ($n = 80$), renal adenocarcinoma ($n = 359$), liver hepatocellular carcinoma ($n = 442$), lung adenocarcinoma ($n = 1,097$), lymphoid neoplasm ($n = 48$), myeloid neoplasm ($n = 200$), ovarian epithelial tumor ($n = 606$), pancreatic adenocarcinoma ($n = 186$), mesothelioma ($n = 87$), prostate adenocarcinoma ($n = 499$), cutaneous melanoma ($n = 479$), sarcoma ($n = 265$), testicular germ cells cancer ($n = 156$), thymic epithelial tumor ($n = 124$), thyroid carcinoma ($n = 516$), endometrial carcinoma ($n = 605$).

The cutaneous melanoma dataset for KP related analyses in melanoma patients was comprised of mRNA-seq data (data accessed at cBioPortal for Cancer Genomics in December 2017, <http://www.cbioportal.org/>) (**Supplementary Table 2**). Survival analyses were correlated with alterations (mutation, amplification, and deletion) in KP-related genes.

Human Protein Atlas Analysis

Human protein atlas has been used for protein and RNA expression analyses of kynurenine pathway-related genes. The protein expression score is based on immunohistochemistry staining and is assigned manually by annotators (<https://www.proteinatlas.org/about/assays+annotation#ihk>), and the RNA-seq quantification data information is found here: <https://www.proteinatlas.org/about/assays+annotation#rna>). Image available from [proteinatlas.org](http://www.proteinatlas.org).

Statistical Analysis

Principal component analysis (PCA) was computed using FactorMineR package for PCA <https://cran.r-project.org/web/packages/FactorMineR/index.html>. KPMs concentration of healthy, PRE and TRM groups was used for PCA. A *t*-test

was used to compare KPMs in two groups of CMM patients. The adjustment methods include the Bonferroni correction (“Bonferroni”) in which the *p*-values are multiplied by the number of comparisons. All *P*-values were two-sided. All analyses were performed using R Statistical Software or Qlucore v3.2 (Qlucore, Lund, Sweden) bioinformatic software.

Network Analysis

In the correlation network analysis, a node represents a KPMs or immune-related biomarker, and an edge is defined by statistically significant correlations between biomarkers in analyses of pre-treatment (PRE) samples. These values (cut-off of 0.5; is the highest level of correlation for which the network is not fragmented) were used to reconstruct networks in PRE and TRM CMM groups (before and during treatment) (49). We defined hubs as nodes with a high degree of centrality (high connectivity with other nodes) in PRE and TRM network. Nodes with a degree higher than the 80th percentile were considered as hubs. Network analysis was carried out with the network analysis tool of a cytoscope (3.4.0).

RESULTS

Differential Expression of Kynurenine Pathway Enzymes Is Associated With Poor Survival in Patients With CMM

To gain further insight into mutations, copy-number alterations, and expression profiles of KP enzymes, we examined the TCGA database (data available at cBioportal.org). The TCGA melanoma cohort consists of 479 samples, and nearly 70% of them were CMM, stage II, and III from patients with no neoadjuvant therapy before tumor resection (Supplementary Table 2). Our analysis showed that within the TCGA cohort, metastatic melanoma and breast cancer are the top two cancer types with the highest burden of gene alterations in enzymes in the KP (Figure 1B, Supplementary Figure 1A). The highest proportion of KP gene mutations (>20%) were found in melanoma patients (Figure 1B). Within the kynurenine pathway, KAT members have the highest mutation frequency, at >8% (Figure 1C). Besides, we found that genetic alterations of KATs that mediate KYNA production from KYN were associated with a reduced survival rate in melanoma patients in the TCGA cohort (Figure 1D).

Further investigation using the Human Protein Atlas, CBio portal in healthy skin and CMM lesions (stage III and IV), show more abundant mRNA/protein expression of CCBL1 and CCBL2 among other KATs (Supplementary Figures 2A–C). Importantly, CCBL1 alteration is correlated to poor prognosis in CMM patients ($p < 0.001$), while KYNU is associated with a better outcome ($p < 0.05$), which can suggest that the KP enzymes possess a different intrinsic mechanism of action (Supplementary Figure 1B). Expression of KMO is not detected in healthy skin, as previously reported (50) or melanoma tumors; while the protein expression of KYNU is lower compared to CCBL1 and CCBL2 both in healthy skin and melanoma tumors (Supplementary Figures 2B,C).

Additional analyses by using a TCGA cohort was processed by the Broad Institute’s pipeline (Firehose run “28 January 2016”: doi: 10.7908/C11G0KM9) consisting of 368 CMM samples showing that BRAF-mutant tumors retain distinct KP gene expression profiles compared to those with wild-type BRAF (Supplementary Figure 9, Supplementary Table 3). This result may suggest the existence of an association between BRAF mutation background and altered mRNA expression of KP members.

Kynurenine Pathway Metabolite Profiles in PRE and TRM Metastatic CMM Patients Is Compared to Healthy Controls

In order to explore how KP alteration in tumor biopsies reflected in the plasma and to further characterize the role of KP in CMM patients, we performed LC-MS/MS metabolite analysis on plasma samples derived from metastatic CMM patients, before (PRE) and during the first treatment (TRM) with MAPKIs ($n = 5$). Besides, plasma samples of five healthy volunteers were included in this comparison as controls. A total of seven metabolites, including TRP, KYN, KYNA, 3-HK, AA, 3HAA, and XA, were analyzed. The influence of confounding factors such as gender and, age on KP metabolite concentrations was compared between CMM patients and healthy controls using a principal component analysis (PCA) (Supplementary Figure 3). Our results were thus not affected by these confounders; therefore, they were not corrected in further analysis. Metabolic profile analyses revealed significantly lower 3-HK ($p < 0.001$) and 3HAA ($p < 0.001$) levels in PRE CMM-patients compared to healthy controls (Table 2, Figures 2A,B). Moreover, clinical intervention by MAPKIs was associated with increased concentrations of 3-HK and 3HAA in TRM plasma samples (Table 2, Figures 2A,B). These results suggest that 3-HK and 3HAA levels may serve as Predictive metabolites in CMM.

Besides, a higher 3-HK/KYN ratio in healthy individuals indicates that more KYN metabolizes toward 3-HK in healthy controls compared to CMM patients. On the other hand, a higher XA/3-HK ratio was observed in melanoma patients, suggesting the higher activity of the KAT II enzyme, which mediates the metabolism of 3-HK toward XA. Collectively, this result proposes that melanoma patients may have a higher accumulation of KYN and a lower concentration of 3-HK and 3HAA in the plasma. Therefore, KP possesses a different trajectory and path in healthy individuals compared with CMM patients (Supplementary Figure 6).

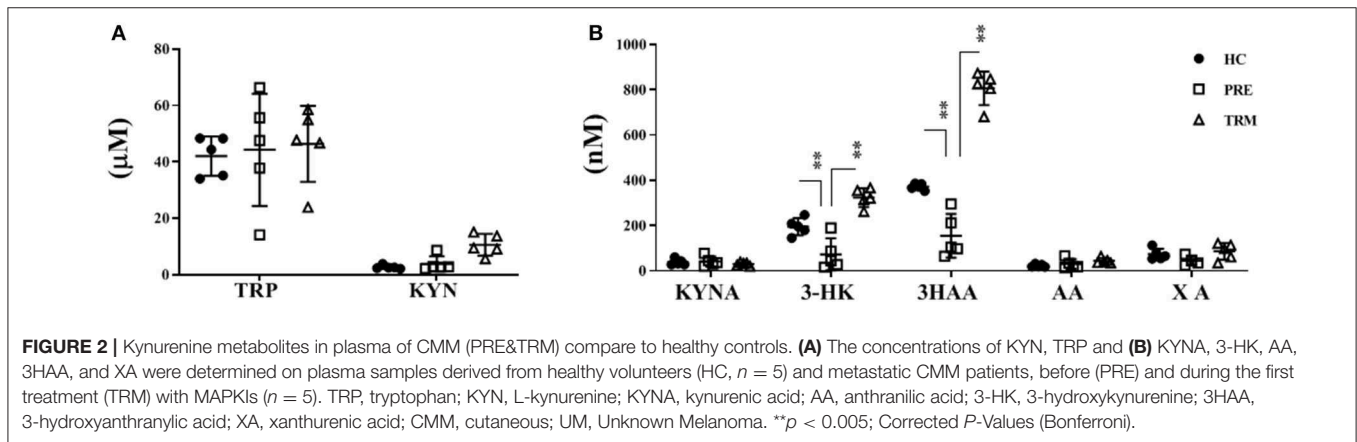
MAPKIs Treatment and Association With Divergent Kynurenine Pathway Activities: Comparison of the Correlation Network in PRE and TRM Groups

In the patient group, we evaluated whether there is an association between treatment and altered KPM concentrations/selected human plasma proteins (measured by LC-MS/MS and PEA using Olink® ImmunoOnc I panel, respectively) in PRE and TRM samples. The selected immuno-oncology PEA panel includes proteins involved in processes such as

TABLE 2 | Kynurenine metabolites in plasma of CMM (PRE&TRM) compare to healthy controls.

	Healthy control (n = 5)	95% IC	PRE (mean n = 5)	95% IC	Corrected P-value (healthy vs. PRE)	TRM (mean n = 5)	95% IC	Corrected P-value (PRE vs. TRM)
TRP (μM)	42.04	35.9–48.2	45.4	34.0–58.7	>0.9999	42.98	31.2–54.7	>0.9999
KYN (μM)	2.66	2.1–3.3	3.54	1.8–5.2	>0.9999	9.78	6.6–12.9	0.9374
KYNA (nM)	38.11	26.0–50.2	43.45	24.0–55.1	0.9880	27.57	19.8–35.4	0.9051
3-HK (nM)	195.30	162.6–228.0	73.23	21.9–111.2	<0.001**	324.9	295.6–354.2	<0.001**
3HAA (nM)	372.28	360.3–384.3	147.96	77.9–218.0	<0.001**	804.47	751.2–857.8	<0.001**
AA (nM)	23.10	17.9–28.3	28.51	13.1–40.5	0.3793	43.85	35.4–52.3	0.7467
XA (nM)	73.51	52.0–95.0	57.23	25.8–77.8	0.5776	88.51	62.1–115.0	0.3203

TRP, tryptophan; KYN, L-kynurenine; KYNA, kynurenic acid; AA, anthranilic acid; 3-HK, 3-hydroxykynurenine; 3HAA, 3-hydroxyanthranilic acid; XA, xanthurenic acid (XA); CMM, cutaneous; UM, Unknown Melanoma. ** $p < 0.005$; Corrected P-Values (Bonferroni).



tumor promotion/suppression, tumor immunity, chemotaxis, vascular and tissue remodeling, apoptosis and cell killing and, metabolism. Reconstruction of correlation networks using Spearman correlation coefficient analyses were performed on plasma immune-related proteins and KPMs in PRE (Supplementary Tables 5, 7) and TRM groups (Supplementary Tables 6, 8). In this analysis, a node represents a KPM or immune-related biomarker, and an edge is defined by statistically significant correlations between biomarkers using correlation analyses. These values (cut-off: Spearman correlation ≥ 0.5 ; this is the highest level of correlation in which a network is not fragmented) were used to reconstruct networks in PRE and TRM CMM groups (49). Compared to the PRE network, the TRM network had more edges and higher median degree (Table 3A, Figures 3B,C, Supplementary Figure 7), which means nodes in TRM network tended to have a higher degree than those in the PRE-network ($p = 0.007$ based on a K-S test, Supplementary Figure 4A). This result indicates that distinct properties of the PRE and TRM network and changes in 3-HK levels in CMM plasma samples were associated with therapeutic intervention by MAPKIs. The median degree value was 4.0 in PRE-network and 6.0 in the TRM network. The total number of edges was significantly higher in the TRM network ($n = 253$) than in the PRE-network ($n = 178$) in a permutation test ($p < 0.0001$, Table 3,

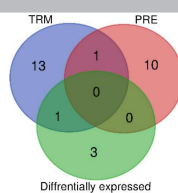
Supplementary Figure 4B). 3-HK has the highest number of connections in PRE and tended to lose interactions in the TRM group (Figure 4A).

On the other hand, AA and KYNA have the highest number of connections among the KPMs in the TRM network (Figures 4B,C). The value of the average clustering coefficient was 0.46 in the PRE network and 0.51 in the TRM network, indicating greater clustering tendency of the TRM network (Table 3). Together, 3-HK and KYNA interactions in the PRE-network identify the groups of proteins involved in the angiopoietin receptor Tie2 and the tyrosine phosphatase SHP2 signaling. Tie2 and SHP2 have inhibitory effect on Th1 differentiation (51–54); analysis was done by using functional annotation analysis of these sets of proteins with all gene sets in the Molecular Signatures Database (<http://software.broadinstitute.org/gsea/msigdb/>).

In particular IL-12, CD40, MMP-12, TNFRSF4, AA, CCL19, CXCL10, GZMB, IL12RB1, CD5, CD28, CCL3, CD8A, and CXCL11 were highly connected with other biomarkers in TRM network, but not in PRE-network (Table 3, Figures 3B,C, Supplementary Figures 5A,B). On the other hand, protein expression of KLRD1 ($p < 0.05$) and CXCL11 ($p < 0.05$) were higher than other proteins, measured by the PEA immunology panel, in TRM compared to PRE in CMM samples (Figure 3A, Supplementary Table 4). Despite insignificance of

TABLE 3 | (A) Network characteristics **(B)** the overlapping between the hubs with differentially expressed parameters (PEA & LC-MS/MS) in PRE and TRM groups.

Total (N = 12)	PRE (N = 5)	TRM (N = 5)	
(A)			
Correlation network based on original variables			
Number of nodes	81	82	
Number of edges	178	253	
Median degree	4	6	
Average clustering coefficient	0.46	0.51	
Hubs (degree centrality)	MIC-A(0.13) CASP8(0.06) TNFSF14(0.06) MMP7(0.09) CD70(0.09) CXCL13(0.11) IL-10(0.001) TGFB1(0.06) CCL8(0.05) TIE2(0.05) CXCL5(0.13)	GZMB(0.04) CD5(0.04) CCL19(0.04) TNFSF14(0.04) IL-12(0.14) CCL3(0.14) IL12RB1(0.12) TNFRSF4(0.08) CXCL10(0.03) CD28(0.03) CD40(0.03) AA(0.03) MMP12(0.04) CD8A(0.04) CXCL11(0.04)	
Names	PRE	TRM	Differentially expressed
Total	11	15	4
(B)			
Elements	TIE2 TGFB1 CXCL13 CD70 CASP8 CCL8 MIC-A MMP7 IL-10 CXCL5 TNFSF14	IL-12 CD40 MMP-12 TNFRSF4 AA CCL19 CXCL10 GZMB IL12RB1 CD5 CCL3 CD8A TNFSF14 CXCL11	3-HK KYN KLRD1 CXCL11



Numbers are given of overlapping parameters compared to the total number. Venn diagram represents all shared and all unique markers in each group.

statistical power for the expression of CXCL9, CCL8, GZMA, and CCL3 ($p = 0.06$), the trend of higher expression in the mentioned proteins after treatment, worth attention, and evaluation in larger cohorts. Therefore, the interactions in the TRM network led to the identification of proteins that are involved in processes such as Th1/Th2 differentiation, IL12-mediated signaling events, and Toll-like receptor signaling; as shown by functional annotation

analysis of this sets of proteins with all gene sets in the Molecular Signatures Database (<http://software.broadinstitute.org/gsea/msigdb/>).

Besides, we referred to mass spectrometry-based proteome analysis performed on parental A375 and the MAPKIs-resistant sublines (A375R) (**Supplementary Figures 8B–D, Supplementary Table 9**). These analyses show that KYNU expression was higher A375 cell line.

Furthermore, a set of highly correlated markers with KYNU is involved in activation of mTORC1 signaling pathway in this data sets (**Supplementary Figure 8D**). It is reported that TRP depletion leads to mTORC1 pathway suppression and consequently, cell-cycle arrest and T cell anergy (55–57). Thus, we speculated that the lower KYNU expression in A375R involves in acquisition of resistance to MAPKIs.

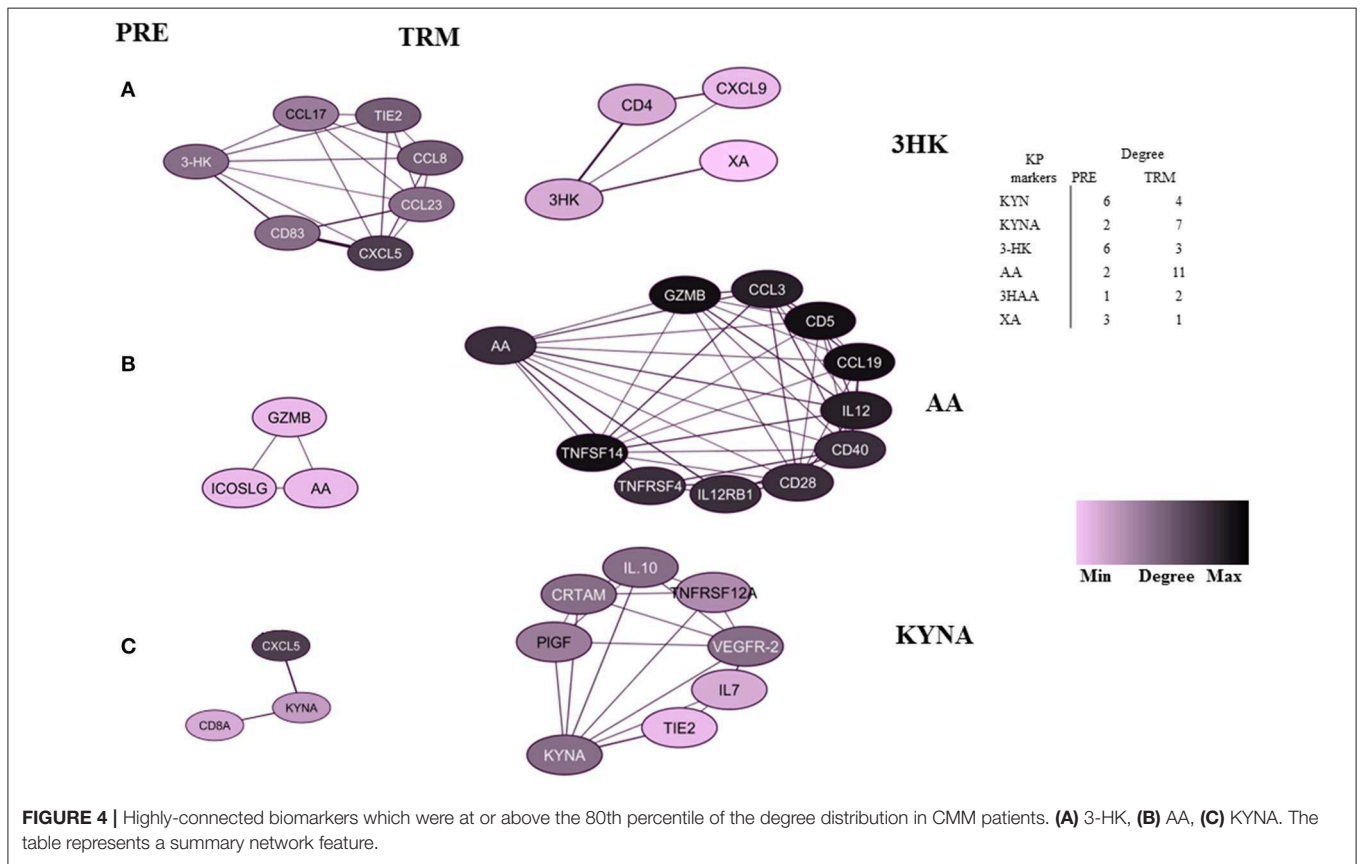
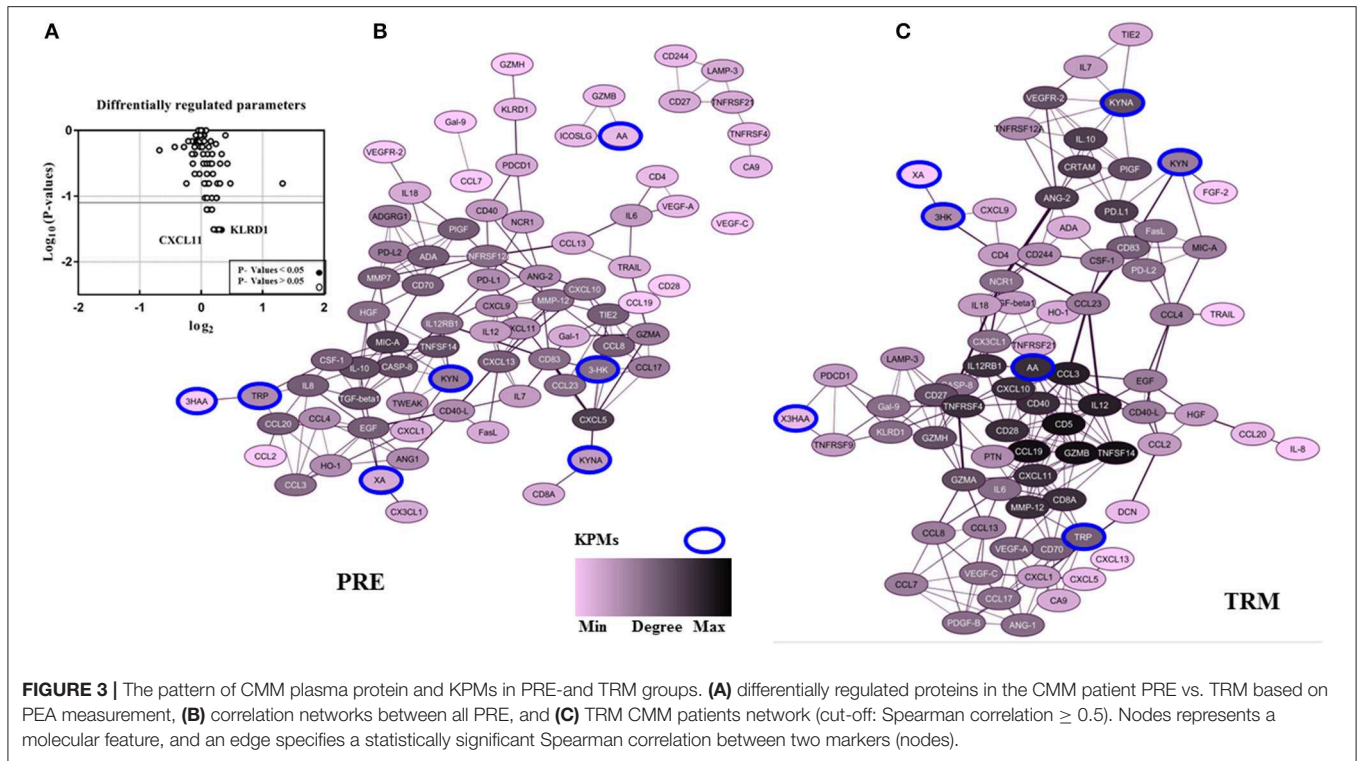
Moreover, we measured the KPMs concentration in A375 and A375R derived medium and cell lysate (**Supplementary Table 10**). Except 3HAA, all KPMs detected in the medium and in the cell lysate only TRP and KYN were detected. However, no differences were detected in the KPMs profile of these two cell lines, nor in the 48 h culture derived medium or in cell lysate (**Supplementary Figure 8A**).

We further investigated the KPM pathway alterations effect on the tumor/ immune cell. We explored whether Th1-cytokines, IFN γ and, TNF- α , can modulate the KYN downstream metabolites such as 3-HK, 3HAA, and AA in cancer cells. For this purpose, melanoma cell lines (A375 and A375R) were treated with IFN γ (50 ng/ml) and TNF- α (10 ng/ml). Although, 3HAA was not detected under these conditions and 3-HK levels was not affected by these cytokines, but IFN γ was able to induce AA in both cell lines (**Supplementary Figure 8A**).

Collectively, these results support that therapeutic intervention by MAPKIs leads to different kynurenine pathways metabolite trajectory which is of importance in altered Th1/Th2 differentiation markers in PRE and TRM CMM groups.

DISCUSSION

Much attention has been dedicated to determining how IDO1, which catalyzes the first and rate-limiting step of TRP degradation, modulates the immune response to tumors. Several clinical trials were designed to combine IDO1 inhibition with ICPIs (7–9). Despite expectations, a recent randomized phase 3 trial combining the IDO1 inhibitor, epacadostat, with pembrolizumab did not show any superior effect compared to pembrolizumab monotherapy in metastatic melanoma (10). This result indicates that the interplay between kynurenine biology and cancer is more complicated than was previously assumed. Besides decreased tryptophan/kynurenine ratio that has been associated with worse prognosis in several cancer types (58, 59), KP downstream metabolites could also play a role in tumoural immune escape. Therefore, inhibition of other components of the KP should be investigated in cancer therapy. Also, the complex interplay of the activity of the KP component may imply the existence of a feedback mechanism; e.g., KMO activity is one determinant of KYNA production by regulating the amount of



KYN substrate available to KATs (60). However, the role of the KPMs, such as KYNA, 3-HK, and AA needs to be investigated further in cancers.

In this study, the cBioPortal with several hundreds of tumor biopsies obtained from different cancer types, including CMM, has been used. Intra-tumoural genetic alterations in KP enzymes have been reported in various cancer types. We also found that CMM and breast cancer patients have the highest KP related genes alteration. Moreover, CMM has the highest rate of KP mutations (>20%), specifically in KATs. Among KATs, CCBL2 is associated with poor survival in CMM patients. Furthermore, BRAF-mutant CMM retains distinct kynurenine pathway-related gene expression profiles compared to BRAF wild type, which suggests the existence of an association between mutation background and kynurenine pathway expression profiles.

Besides, we showed that KP metabolism is altered in PRE and TRM samples from CMM patients treated with MAPKIs, as reflected by changes in plasma levels of downstream metabolites. These new findings raise the question of whether altered kynurenine metabolism is a mean by which CMM cells escape immune attack. Interestingly, an altered ratio of KYNA: 3-HK was reported previously as an indicator of KP modulation in neurodegenerative disorders (61, 62).

By using correlation networks between KPMs and immune parameters, we identified 3-HK, AA, and KYNA as central nodes in network diagrams built around data from PRE and TRM patient samples. 3-HK and KYNA interactions in the PRE network identify groups of proteins such as CXCL13, IL-8, TIE2, ADGRG1, CCL20, and CXCL9 to be involved in Tie2 and SHP2 signaling with an inhibitory effect on Th1 differentiation (51–54). Interaction of Tie2, a tyrosine kinase receptor, with its ligand angiopoietin-1 (Ang1), regulates angiogenesis which makes it an attractive target for cancer therapy (53). Furthermore, Ang1-Tie2 signaling suppresses T cell activation and promotes regulatory T cell expansion (52). Also, Tie2 regulation is involved in Th1 and CD8 immune responses (54). The tyrosine-protein phosphatase non-receptor type 11 (PTPN11), also known as SHP-2, is a critical intracellular regulator that mediates cell proliferation and differentiation (63). It is reported that SHP-2 suppresses Th1 immunity in the tumor microenvironment via the PD-1/SHP-2/STAT1/T-bet signaling axis (51).

On the other hand, correlation network analyses of samples from the same CMM patients showed that the TRM network was denser than the PRE network. Moreover, this analysis led to identification of proteins (CXCL11, IL-12, CD40, MMP-12, TNFRSF4, AA, CCL19, CXCL10, GZMB, IL12RB1, CD5, CD28, CCL3, and CD8A) to be highly connected with other biomarkers which are functionally enriched in processes such as Th1/Th2 regulatory switch, IL12-mediated signaling events and Toll-like receptor signaling.

These observations reveal the relative contribution of these proteins in T cell responses and show an association between higher 3-HK levels and CXCL11 and KLRD1 protein expression in CMM. CXCL11 itself is among the hubs in the TRM network (**Table 3**) and is a T cell activation marker. 3-HK is also connected to CD4+ and CXCL9 in TRM groups, the two factors that are involved in IL-23 signaling CXCL9 and CXCL10

also mediate the suppression of human CD4+ T cell activation by 3, 4-dimethoxycinnamonyl-anthranilic acid (tranilast) (64). While, KYNA connection to IL10, IL-7, and TNFRSF12A in TRM samples suggest an immune-regulatory role for KYNA (65, 66).

Additionally, higher expression of KYNU in A375 cell line compared with A375R was detected. Similarly, a set of highly correlated markers with KYNU is involved in the activation of mTORC1 signaling pathway, which plays a substantial role in the cell cycle and T cell proliferation (55–57).

Together, KP related enzymatic alteration in CMM tumor biopsies is associated with lower plasma level of 3-HK and 3HAA. MAPKIs therapy lead to induction of the 3-HK and 3HAA and is associated with Th1-like response.

Despite the small sample size, this is the first study that has assessed plasma KPMs-Immuno-oncology profiling of CMM patients. However, it is previously reported that lower level of KMO, 3-HK, and 3HAA is associated with less proliferative and exhausted CD4+ T-cells (67). In addition, Lee et al. presented a mild 3-HK increase is critical for cell death commitment and protects mitochondrial function, while more pronounced 3-HK increase induces the dysfunction of mitochondria and activate the apoptotic pathway (68). They additionally showed that 3-HK treatment reduced cell viability and co-treatment with ERK pathway inhibitor, PD98059, synergized in cell death induction. Similarly, active ERK decreased 3-HK induced-neural cell death and inhibition of ERK by specific ERK pathway inhibitor (PD98059) significantly impaired the 3-HK-induced cell death (68).

It is also reported that KYN potentiates the activity of the MAPK-ERK1/2 pathway (69), and inhibition of the MAPK pathway increases the serum levels of IFN γ and TNF- α (70). IFN- γ and TNF- α also induce KMO, KYNU expression as well as 3-HK production (71, 72). Therefore, we speculated that inhibition of MAPK pathway with MAPKIs impair the balance between MAPK pathways with KP activity and therefore activates compensatory feedback loops to elevate KP activation toward 3-HK and 3-HAA production.

Thus, the reduced KYNU expression in MAPKIs-resistant cell line (A375R) suggests that, this may be the rate-limiting step for the utilization of kynurenine. KYN directly activates aryl hydrocarbon receptors, resulting in the activation of immunosuppressive agents (19). Besides, strengthening KMO or KYNU activity leads to the utilization of KYN, and decreasing the excess amount of KYN in the plasma triggers immune evasion, a result that could restore immune surveillance (19). Hence, we speculate that treatments targeting KMO or KYNU may restore antitumor immunity.

However, our result contradicts those reports where the accumulation of KPMs such as 3-HK and 3HAA mediated cell apoptosis in T- B- and natural killer cells (NK) (25). Alternatively, Fallarino et al. reported that 3HAA would induce selective apoptosis in Th1 but not Th2 cells (73). They also suggest that the selective effects of KPMs on T cell apoptosis is not only are required for the maintenance of T cell homeostasis and self-tolerance, but also initiate specific disease conditions through an imbalanced T helper response, which does not necessarily disagree with our results.

In conclusion, this study provides a paradigm to investigate further how the many and seemingly different activities of KMPs could be expanded to accommodate a critical and possibly unifying role in immune regulation in CMM patient.

DATA AVAILABILITY STATEMENT

All datasets generated for this study are included in the article/**Supplementary Material**.

ETHICS STATEMENT

The studies involving human participants were reviewed and approved by the sample collection was conducted by Good Clinical Practice/the Declaration of Helsinki with informed consent from all patients and was approved by the Stockholm Regional Ethics Committee, Karolinska Institute, Sweden. The patients/participants provided their written informed consent to participate in this study.

AUTHOR CONTRIBUTIONS

SR and JT: design, conception, and developed the methodology. SR, HM, NK, DG-C, and JT: analyzed and interpreted the data.

AH, XZ, and DM: performed the HILIC-MS/MS. MP and JL: PEA data. SR, HM, NK, DG-C, AH, MP, JL, XZ, DM, HE, JH, and JT: writing and reviewing of the manuscript.

FUNDING

This work was supported by the Karolinska Institute's faculty funds for doctoral education (KID); VINNMER Marie Curie Incoming fellowship, VR (Scientific Research Council); ERC (ID nr C0493601); KA Wallenberg Foundation (KAW 2017.0077 to JT).

ACKNOWLEDGMENTS

We thank Peri Noori, the laboratory managers, and all the lab members for their valuable comments. We thank Pernilla Appelquist for their editorial support.

SUPPLEMENTARY MATERIAL

The Supplementary Material for this article can be found online at: <https://www.frontiersin.org/articles/10.3389/fonc.2020.00051/full#supplementary-material>

REFERENCES

- Ward WH, Farma JM. (eds.). (2017). *Cutaneous Melanoma: Etiology and Therapy*. Philadelphia, PA: Codon Publications.
- Zhou AY, Johnson DB. Combinatorial therapies in melanoma: MAPK inhibitors and beyond. *Am J Clin Dermatol.* (2018) 19:181–93. doi: 10.1007/s40257-017-0320-y
- Robert C, Long GV, Brady B, Dutriaux C, Maio M, Mortier L, et al. Nivolumab in previously untreated melanoma without BRAF mutation. *N Engl J Med.* (2015) 372:320–30. doi: 10.1056/NEJMoa1412082
- Leung AM, Lee AF, Ozao-Choy J, Ramos RI, Hamid O, O'Day SJ, et al. Clinical benefit from ipilimumab therapy in melanoma patients may be associated with serum CTLA4 levels. *Front Oncol.* (2014) 4:10. doi: 10.3389/fonc.2014.00110
- Robert C, Schachter J, Long GV, Arance A, Grob JJ, Mortier L, et al. Pembrolizumab versus ipilimumab in advanced melanoma. *N Engl J Med.* (2015) 372:2521–32. doi: 10.1056/NEJMoa1503093
- Wolchok JD, Chiarion-Sileni V, Gonzalez R, Rutkowski P, Grob JJ, Cowey CL, et al. Overall survival with combined nivolumab and ipilimumab in advanced melanoma. *N Engl J Med.* (2017) 377:1345–56. doi: 10.1056/NEJMoa1709684
- Gangadhar TC, Hamid O, Smith DC, Bauer TM, Wasser JS, Luke JJ, et al. Preliminary results from a Phase I/II study of epacadostat (incb024360) in combination with pembrolizumab in patients with selected advanced cancers. *J Immuno Therapy Cancer.* (2015) 3:O7. doi: 10.1186/2051-1426-3-S2-O7
- Zakharia Y, Drabick JJ, Khleif S, McWilliams RR, Munn D, Link CJ, et al. Updates on phase 1b/2 trial of the indoleamine 2,3-dioxygenase pathway (IDO) inhibitor indoximod plus checkpoint inhibitors for the treatment of unresectable stage 3 or 4 melanoma. *J Clin Oncol.* (2016) 34(15_suppl):3075. doi: 10.1200/JCO.2016.34.15_suppl.3075
- Marin-Acevedo JA, Dholaria B, Soyano AE, Knutson KL, Chumsri S, Lou Y. Next generation of immune checkpoint therapy in cancer: new developments and challenges. *J Hematol Oncol.* (2018) 11:39. doi: 10.1186/s13045-018-0582-8
- Long GV, Dummer R, Hamid O, Gajewski T, Caglevic C, Dalle S, et al. Epacadostat (E) plus pembrolizumab (P) versus pembrolizumab alone in patients (pts) with unresectable or metastatic melanoma: results of the phase 3 ECHO-301/KEYNOTE-252 study. *J Clin Oncol.* (2018) 36(15_Suppl):108. doi: 10.1016/S1470-2045(19)30274-8
- Marincola FM, Bedognetti D, Roelands J, Decock J, Wang E, Hendrickx W. The MAPK hypothesis: immune-regulatory effects of MAPK-pathway genetic dysregulations and implications for breast cancer immunotherapy. *Emerg Top Life Sci.* (2017) 1:429–45. doi: 10.1042/ETLS20170142
- Ascierto PA, Dummer R. Immunological effects of BRAF+MEK inhibition. *Oncoimmunology.* (2018) 7:e1468955. doi: 10.1080/2162402X.2018.1468955
- Donia M, Fagone P, Nicoletti F, Andersen RS, Høgdall E, Straten PT, et al. BRAF inhibition improves tumor recognition by the immune system: potential implications for combinatorial therapies against melanoma involving adoptive T-cell transfer. *Oncoimmunology.* (2012) 1:1476–83. doi: 10.4161/onci.21940
- Sapkota B, Hill CE, Pollack BP. Vemurafenib enhances MHC induction in BRAF(V600E) homozygous melanoma cells. *Oncoimmunology.* (2013) 2:e22890. doi: 10.4161/onci.22890
- Frederick DT, Piris A, Cogdill AP, Cooper ZA, Lezcano C, Ferrone CR, et al. BRAF inhibition is associated with enhanced melanoma antigen expression and a more favorable tumor microenvironment in patients with metastatic melanoma. *Clin Cancer Res.* (2013) 19:1225–31. doi: 10.1158/1078-0432.CCR-12-1630
- Sumimoto H, Imabayashi F, Iwata T, Kawakami Y. The BRAF-MAPK signaling pathway is essential for cancer-immune evasion in human melanoma cells. *J Exp Med.* (2006) 203:1651–6. doi: 10.1084/jem.20051848
- Yu C, Liu X, Yang J, Zhang M, Jin H, Ma X, et al. Combination of immunotherapy with targeted therapy: theory and practice in metastatic melanoma. *Front Immunol.* (2019) 10:90. doi: 10.3389/fimmu.2019.00990
- Brummer C, Faerber S, Bruss C, Blank C, Lacroix R, Haferkamp S, et al. Metabolic targeting synergizes with MAPK inhibition and delays drug resistance in melanoma. *Cancer Lett.* (2019) 442:53–463. doi: 10.1016/j.canlet.2018.11.018
- Badawy AA. Kynurenine pathway of tryptophan metabolism: regulatory and functional aspects. *Int J Tryptophan Res.* (2017) 10:178646917691938. doi: 10.1177/1178646917691938

20. Darlington LG, Mackay GM, Forrest CM, Stoy N, George C, Stone TW. Altered kynurenine metabolism correlates with infarct volume in stroke. *Eur J Neurosci.* (2007) 26:2211–21. doi: 10.1111/j.1460-9568.2007.05838.x
21. Lim CK, Yap MM, Kent SJ, Gras G, Samah B, Batten JC, et al. Characterization of the kynurenine pathway and quinolinic Acid production in macrophages. *Int J Tryptophan Res.* (2013) 6:7–19. doi: 10.4137/IJTR.S11789
22. Sathyasaikumar KV, Stachowski EK, Wonodi I, Roberts RC, Rassoulpour A, McMahon RP, et al. Impaired kynurenine pathway metabolism in the prefrontal cortex of individuals with schizophrenia. *Schizophr Bull.* (2011) 37:1147–56. doi: 10.1093/schbul/sbj112
23. Baran H, Jellinger K, Deecke L. Kynurenine metabolism in Alzheimer's disease. *J Neural Transm.* (1999) 106:165–81. doi: 10.1007/s007020050149
24. Midttun O, Townsend MK, Nygård O, Tweroger SS, Brennan P, Johansson M, et al. Most blood biomarkers related to vitamin status, one-carbon metabolism, and the kynurenine pathway show adequate preanalytical stability and within-person reproducibility to allow assessment of exposure or nutritional status in healthy women and cardiovascular patients. *J Nutr.* (2014) 144:784–90. doi: 10.3945/jn.113.189738
25. Baumgartner R, Forteza MJ, Ketelhuth DFJ. The interplay between cytokines and the Kynurenine pathway in inflammation and atherosclerosis. *Cytokine.* (2019) 122:154148. doi: 10.1016/j.cyto.2017.09.004
26. Ball HJ, Sanchez-Perez A, Weiser S, Austin CJD, Astelbauer F, Miu J, et al. Characterization of an indoleamine 2,3-dioxygenase-like protein found in humans and mice. *Gene.* (2007) 396:203–13. doi: 10.1016/j.gene.2007.04.010
27. Metz R, Duhadaway JB, Kamasani U, Laury-Kleintop L, Muller AJ, Prendergast GC. Novel tryptophan catabolic enzyme IDO2 is the preferred biochemical target of the antitumor indoleamine 2,3-dioxygenase inhibitory compound D-1-methyl-tryptophan. *Cancer Res.* (2007) 67:7082–7. doi: 10.1158/0008-5472.CAN-07-1872
28. Yuasa HJ, Takubo M, Takahashi A, Hasegawa T, Noma H, Suzuki T. Evolution of vertebrate indoleamine 2,3-dioxygenases. *J Mol Evol.* (2007) 65:705–14. doi: 10.1007/s00239-007-9049-1
29. Han Q, Cai T, Tagle DA, Li J. Structure, expression, and function of kynurenine aminotransferases in human and rodent brains. *Cell Mol Life Sci.* (2009) 67:353–68. doi: 10.1007/s00018-009-0166-4
30. Amaral M, Levy C, Heyes DJ, Lafite P, Outeiro TF, Giorgini F, et al. Structural basis of kynurenine 3-monoxygenase inhibition. *Nature.* (2013) 496:382–5. doi: 10.1038/nature12039
31. Schwarcz R, Bruno JP, Muchowski PJ, Wu H-Q. Kynurenines in the mammalian brain: when physiology meets pathology. *Nat Rev Neurosci.* (2012) 13:465–77. doi: 10.1038/nrn3257
32. Ino K, Yamamoto E, Shibata K, Kajiyama H, Yoshida N, Terauchi M, et al. Inverse correlation between tumoral indoleamine 2,3-dioxygenase expression and tumor-infiltrating lymphocytes in endometrial cancer: its association with disease progression and survival. *Clin Cancer Res.* (2008) 14:2310–7. doi: 10.1158/1078-0432.CCR-07-4144
33. Suzuki Y, Suda T, Furuhashi K, Suzuki M, Fujie M, Hahimoto D, et al. Increased serum kynurenine/tryptophan ratio correlates with disease progression in lung cancer. *Lung Cancer.* (2010) 67:361–5. doi: 10.1016/j.lungcan.2009.05.001
34. Yoshida N, Ino K, Ishida Y, Kajiyama H, Yamamoto E, Shibata K, et al. Overexpression of indoleamine 2,3-dioxygenase in human endometrial carcinoma cells induces rapid tumor growth in a mouse xenograft model. *Clin Cancer Res.* (2008) 14:7251–9. doi: 10.1158/1078-0432.CCR-08-0991
35. Chung KT, Gadupudi GS. Possible roles of excess tryptophan metabolites in cancer. *Environ Mol Mutagen.* (2011) 52:81–104. doi: 10.1002/em.20588
36. Juhász C, Muzik O, Lu X, Jahania MS, Soubani AO, Khalaf M, et al. Quantification of tryptophan transport and metabolism in lung tumors using PET. *J Nucl Med.* (2009) 50:356–63. doi: 10.2967/jnumed.108.058776
37. Tankiewicz A, Dziedzianczyk D, Buczek P, Szarmach IJ, Grabowska SZ, Pawlak D. Tryptophan and its metabolites in patients with oral squamous cell carcinoma: preliminary study. *Adv Med Sci.* (2006) 51(Suppl. 1):21–4.
38. Sordillo PP, Sordillo LA, Helson L. The Kynurenine Pathway: a primary resistance mechanism in patients with glioblastoma. *Anticancer Res.* (2017) 37:2159–71. doi: 10.21873/anticancer.11551
39. Liu M, Wang X, Wang L, Ma X, Gong Z, Zhang S, et al. Targeting the IDO1 pathway in cancer: from bench to bedside. *J Hemato Oncol.* (2018) 11:100. doi: 10.1186/s13045-018-0644-y
40. Adams JL, Smothers J, Srinivasan R, Hoos A. Big opportunities for small molecules in immuno-oncology. *Nat Rev Drug Discov.* (2015) 14:603–22. doi: 10.1038/nrd4596
41. Clara RO, Assmann N, Ramos Moreno AC, Coimbra JB, Nurenberger N, Dettmer-Wilde K, et al. Melanocytes are more responsive to IFN- γ and produce higher amounts of kynurenine than melanoma cells. *Biol Chem.* (2016) 397:85–90. doi: 10.1515/hsz-2015-0173
42. Xie DL, Wu J, Lou YL, Zhong XP. Tumor suppressor TSC1 is critical for T-cell anergy. *Proc Natl Acad Sci USA.* (2012) 109:14152–7. doi: 10.1073/pnas.1119744109
43. Metz R, Rust S, Duhadaway JB, Mautino MR, Munn DH, Vahanian NN, et al. IDO inhibits a tryptophan sufficiency signal that stimulates mTOR: A novel IDO effector pathway targeted by D-1-methyl-tryptophan. *Oncimmunology.* (2012) 1:1460–8. doi: 10.4161/onci.21716
44. Banzola I, Mengus C, Wyler S, Hudolin T, Manzella G, Chiarugi A, et al. Expression of indoleamine 2,3-dioxygenase induced by IFN-gamma and TNF-alpha as potential biomarker of prostate cancer progression. *Front Immunol.* (2018) 9:1051. doi: 10.3389/fimmu.2018.01051
45. Speckaert R, Vermaelen K, van Geel N, Autier P, Lambert J, Haspeslagh M, et al. Indoleamine 2,3-dioxygenase, a new prognostic marker in sentinel lymph nodes of melanoma patients. *Eur J Cancer.* (2012) 48:2004–11. doi: 10.1016/j.ejca.2011.09.007
46. Heng B, Lim CK, Lovejoy DB, Bessede A, Gluch L, Guillemin GJ. Understanding the role of the kynurenine pathway in human breast cancer immunobiology. *Oncotarget.* (2016) 7:6506–20. doi: 10.18632/oncotarget.6467
47. Azimi A, Tuominen R, Costa Svedman F, Caramuta S, Pernemalm M, Frostvik Stolt M, et al. Silencing FLI or targeting CD13/ANPEP lead to dephosphorylation of EPHA2, a mediator of BRAF inhibitor resistance, and induce growth arrest or apoptosis in melanoma cells. *Cell Death Dis.* (2017) 8:e3029. doi: 10.1038/cddis.2017.406
48. Assarsson E, Lundberg M, Holmquist G, Björkstén J, Thorsen SB, Ekman D, et al. Homogenous 96-plex PEA immunoassay exhibiting high sensitivity, specificity, and excellent scalability. *PLoS ONE.* (2014) 9:e95192. doi: 10.1371/journal.pone.0095192
49. Kiani NA, Zenil H, Olczak J, Tegnér J. Evaluating network inference methods in terms of their ability to preserve the topology and complexity of genetic networks. *Semin Cell Dev Biol.* (2016) 51:4–52. doi: 10.1016/j.semcdb.2016.01.012
50. Fagerberg L, Hallström BM, Oksvold P, Kampf C, Djureinovic D, Odeberg J, et al. Analysis of the human tissue-specific expression by genome-wide integration of transcriptomics and antibody-based proteomics. *Mol Cell Proteomics.* (2014) 13:397–406. doi: 10.1074/mcp.M113.035600
51. Li J, Jie HB, Lei Y, Gildener-Leapman N, Trivedi S, Green T, et al. PD-1/SHP-2 inhibits Tc1/Th1 phenotypic responses and the activation of T cells in the tumor microenvironment. *Cancer Res.* (2015) 75:508–18. doi: 10.1158/0008-5472.CAN-14-1215
52. Coffelt SB, Chen YY, Muthana M, Welford AF, Tal AO, Scholz A, et al. Angiotensin 2 stimulates TIE2-expressing monocytes to suppress T cell activation and to promote regulatory T cell expansion. *J Immunol.* (2011) 186:4183–90. doi: 10.4049/jimmunol.1002802
53. Grenga I, Kwilas AR, Donahue RN, Farsaci B, Hodge JW. Inhibition of the angiotensin/Tie2 axis induces immunogenic modulation, which sensitizes human tumor cells to immune attack. *J Immunother Cancer.* (2015) 3:2. doi: 10.1186/s40425-015-0096-7
54. Soong L. Dysregulated Th1 immune and vascular responses in scrub typhus pathogenesis. *J Immunol.* (2018) 200:1233–40. doi: 10.4049/jimmunol.1701219
55. Munn DH, Sharma MD, Baban B, Harding HP, Zhang Y, Ron D, et al. GCN2 kinase in T cells mediates proliferative arrest and anergy induction in response to indoleamine 2,3-dioxygenase. *Immunity.* (2005) 22:633–42. doi: 10.1016/j.immuni.2005.03.013
56. Eleftheriadis T, Pissas G, Antoniadis G, Liakopoulos V, Stefanidis I. Indoleamine 2,3-dioxygenase depletes tryptophan, activates general control non-repressible 2 kinase and down-regulates key enzymes involved in fatty acid synthesis in primary human CD4+ T cells. *Immunology.* (2015) 146:292–300. doi: 10.1111/imm.12502

57. Munn DH, Shafizadeh E, Attwood JT, Bondarev I, Pashine A, Mellor AL. Inhibition of T cell proliferation by macrophage tryptophan catabolism. *J Exp Med.* (1999) 189:1363–72. doi: 10.1084/jem.189.9.1363
58. Wang W, Huang L, Jin JY, Jolly S, Zang Y, Wu H, et al. IDO immune status after chemoradiation may predict survival in lung cancer patients. *Cancer Res.* (2018) 78:809–16. doi: 10.1158/0008-5472.CAN-17-2995
59. Zhai L, Dey M, Lauing KL, Gritsina G, Kaur R, Lukas RV, et al. The kynurenine to tryptophan ratio as a prognostic tool for glioblastoma patients enrolling in immunotherapy. *J Clin Neurosci.* (2015) 22:1964–8. doi: 10.1016/j.jocn.2015.06.018
60. Erhardt S, Pocivavsek A, Repici M, Liu XC, Imbeault S, Maddison DC, et al. Adaptive and behavioral changes in kynurenine 3-monooxygenase knockout mice: relevance to psychotic disorders. *Biol Psychiatry.* (2017) 82:756–65. doi: 10.1016/j.biopsych.2016.12.011
61. Szymona K, Zdzisinska B, Karakula-Juchnowicz H, Kocki T, Kandefer-Szerszen M, Flis M, et al. Correlations of kynurenic acid, 3-hydroxykynurenine, sIL-2R, IFN-alpha, and IL-4 with clinical symptoms during acute relapse of schizophrenia. *Neurotox Res.* (2017) 32:17–26. doi: 10.1007/s12640-017-9714-0
62. Johansson AS, Owe-Larsson B, Asp L, Kocki T, Adler M, Hetta J, et al. Activation of kynurenine pathway in *ex vivo* fibroblasts from patients with bipolar disorder or schizophrenia: cytokine challenge increases production of 3-hydroxykynurenine. *J Psychiatr Res.* (2013) 47:1815–23. doi: 10.1016/j.jpsychires.2013.08.008
63. Freeman RM, Plutzky J, Neel BG. Identification of a human src homology 2-containing protein-tyrosine-phosphatase: a putative homolog of *Drosophila* corkscrew. *Proc Natl Acad Sci USA.* (1992) 89:11239–43. doi: 10.1073/pnas.89.23.11239
64. Hertenstein A, Schumacher T, Litzenburger U, Opitz CA, Falk CS, Serafini T, et al. Suppression of human CD4+ T cell activation by 3,4-dimethoxycinnamonyl-anthranilic acid (tranilast) is mediated by CXCL9 and CXCL10. *Biochem Pharmacol.* (2011) 82:632–41. doi: 10.1016/j.bcp.2011.06.013
65. Mazzucchelli R, Hixon JA, Spolski R, Chen X, Li WQ, Hall VL, et al. Development of regulatory T cells requires IL-7Ralpha stimulation by IL-7 or TSLP. *Blood.* (2008) 112:3283–92. doi: 10.1182/blood-2008-02-137414
66. Asseman C, Mauze S, Leach MW, Coffman RL, Powrie F. An essential role for interleukin 10 in the function of regulatory T cells that inhibit intestinal inflammation. *J Exp Med.* (1999) 190:995–1003. doi: 10.1084/jem.190.7.995
67. Rad Pour S, Morikawa H, Kiani NA, Yang M, Azimi A, Shafi G, et al. Exhaustion of CD4+ T-cells mediated by the kynurenine pathway in melanoma. *Sci Rep.* (2019) 9:12150. doi: 10.1038/s41598-019-48635-x
68. Lee HJ, Bach JH, Chae HS, Lee SH, Joo WS, Choi SH, et al. Mitogen-activated protein kinase/extracellular signal-regulated kinase attenuates 3-hydroxykynurenine-induced neuronal cell death. *J Neurochem.* (2004) 88:647–56. doi: 10.1111/j.1471-4159.2004.02191.x
69. Li Y, Kilani RT, Rahmani-Neishaboore E, Jalili RB, Ghahary A. Kynurenine increases matrix metalloproteinase-1 and -3 expression in cultured dermal fibroblasts and improves scarring *in vivo*. *J Invest Dermatol.* (2014) 134:643–50. doi: 10.1038/jid.2013.303
70. Wilmott JS, Haydu LE, Menzies AM, Lum T, Hyman J, Thompson JF, et al. Dynamics of chemokine, cytokine, and growth factor serum levels in BRAF-mutant melanoma patients during BRAF inhibitor treatment. *J Immunol.* (2014) 192:2505–13. doi: 10.4049/jimmunol.1302616
71. Owe-Young R, Webster NL, Mukhtar M, Pomerantz RJ, Smythe G, Walker D, et al. Kynurenine pathway metabolism in human blood-brain-barrier cells: implications for immune tolerance and neurotoxicity. *J Neurochem.* (2008) 105:1346–57. doi: 10.1111/j.1471-4159.2008.05241.x
72. Mándi Y, Vécsei L. The kynurenine system and immunoregulation. *J Neural Transm.* (2012) 119:197–209. doi: 10.1007/s00702-011-0681-y
73. Fallarino F, Grohmann U, Vacca C, Bianchi R, Orabona C, Spreca A, et al. T cell apoptosis by tryptophan catabolism. *Cell Death Differ.* (2002) 9:1069–77. doi: 10.1038/sj.cdd.4401073

Conflict of Interest: The authors declare that the research was conducted in the absence of any commercial or financial relationships that could be construed as a potential conflict of interest.

Copyright © 2020 Rad Pour, Morikawa, Kiani, Gomez-Cabrero, Hayes, Zheng, Pernemalm, Lehtiö, Mole, Hansson, Eriksson and Tegnér. This is an open-access article distributed under the terms of the Creative Commons Attribution License (CC BY). The use, distribution or reproduction in other forums is permitted, provided the original author(s) and the copyright owner(s) are credited and that the original publication in this journal is cited, in accordance with accepted academic practice. No use, distribution or reproduction is permitted which does not comply with these terms.